Two exactly soluble lattice models in three dimensions

F.Y. Wu

Department of Physics, Northeastern University
Boston, Massachusetts 02115

As a prelude to what might be expected as forthcoming breakthroughs in finding new approaches toward solving three-dimensional lattice models in the twenty-first century, we review the exact solutions of two lattice models in three dimensions obtained using the conventional combinatorial and transfer matrix approaches.

1 Introduction

The twenties century has witnessed the birth and growth of the field of exactly solvable models in statistical mechanics. It began with the Lenz-Ising model of Ising[1] and its solution in two dimensions by Onsager.[2] Beginning in the 1960's the field of exactly solvable models grew phenomenally to encompass vertex-type models[3, 4] and related problems.[5] But most of the new soluble models are limited to two dimensions. To be sure, several three-dimensional systems have been studied with various degrees of success in recent years. They include the Zamolodchikov model [6] solved by Baxter,[7] its more recent extension by Bazhanov and Baxter,[8] and two models solved by this author and collaborators.[9, 10, 11] But these solutions invariably suffer defects of one kind or another, and the prevailing consensus is that the solution of genuine three-dimensional systems must await for major breakthroughs. Before the arrival of the new breakthroughs, however, it is instructive to pause, and examine the usefulness of conventional approaches when applied to three-dimensional systems.

There are generally two conventional approaches, namely, a combinatorial approach using graphical methods including Pfaffians and an algebraic approach using the method of the transfer matrix, both of which have been applied with some success in treating three-dimensional systems. Here, we review two such solutions.[9, 10] It is hoped that, with an understanding of what has been done and what cannot be done with the conventional approaches, one can then proceed ahead to explore new lines of inquiry toward solving genuine three-dimensional lattice models in the twenty-first century.

2 The combinatorial solution of an $O(-1)$ model

2.1 Definition of the model

Consider a simple cubic lattice $\mathcal{L}$ of $\mathcal{N} = N_1 \times N_2 \times N_3$ sites. The partition function of an $O(n)$ model [12, 13] on $\mathcal{L}$ is the graph generating function

$$Z(n) = \sum_{\text{closed polygons}} n^{\ell} z^{b}, \tag{1}$$

where the summation is taken over all closed non-intersecting polygonal configurations on $\mathcal{L}$, ℓ is the number of polygons, and b is the number of edges

contained each configuration. We shall restrict to polygons which are directed in a generally negative to positive direction along the three principal axes, hence a special three-dimensional system. Assuming periodic boundary conditions, the lines will then loop around the lattice, with each loop cutting one or more times a plane perpendicular to the $(1,1,1)$ direction. While the evaluation of (1) for general n is still open, we consider here the $n=-1$ problem and are interested in the per-site partition function, or "free energy",

$$f = \lim_{\mathcal{N}\to\infty} \mathcal{N}^{-1} \ln Z(-1). \tag{2}$$

2.2 Equivalence with a dimer problem

Our strategy is to establish a one-one correspondence between the configurations in (1) and dimer configurations on a related lattice $\mathcal{L}'$, and that the latter can be evaluated as a Pfaffian. To construct $\mathcal{L}'$, we split each lattice point of $\mathcal{L}$ into two, with one point attached to the three positive axes and the other to the three negative axes as shown in Fig. 1. The dimer lattice $\mathcal{L}'$ is then obtained by reconnecting the split pairs with new inserted edges. We shall associate dimer weights z to edges originally in $\mathcal{L}$, and weights 1 to the newly inserted edges as shown.

The one-one correspondence between vertex configurations on $\mathcal{L}$ and dimer configurations on $\mathcal{L}'$ can be seen by superimposing any given dimer configuration C_i with a standard one, C_0, in which all inserted edges are covered by dimers. The superposition of the two dimer configurations produces a graph of transition cycles,[14] or polygons, belonging to one of two kinds: i) double dimers placed on new edges, and ii) line configurations looping around the lattice. In the latter case the line configurations form precisely the same polygonal configurations as in (1). Conversely, to each polygonal configuration in (1), there exists a unique dimer configuration C_i which, when superimposed with C_0, produces the line configuration in question. This establishes the desired correspondence.

Now there are $\mathcal{N}$ sites on $\mathcal{L}$, and this leads us to consider a Pfaffian $\mathrm{Pf}A$ of dimension $2\mathcal{N}$. The convention of fixing signs to lattice edges is to direct edges of $\mathcal{L}'$ such that the element $A_{\alpha\beta}$ is positive (negative) if an edge is directed from site α to β (β to α). We choose to direct all edges of $\mathcal{L}'$ along the positive directions as shown in Fig. 1. Consider a typical term in the Pfaffian corresponding to a dimer configuration C_i. The sign of this term

relative to the term corresponding to C_0 is the product of the signs of the transition cycles produced by the superimposition of C_i and C_0. The rule is that each transition cycle carries a sign $(-1)^{m+1}$, where m is the number of arrows pointing in a given direction when the transition cycle is traversed.[14] For transition cycles consisting of double dimers we have $m = 1$ so that the sign is always positive. For other transition cycles, or loops, we have always $m =$ even, so that each loop carries a factor -1. As a consequence, the relative sign of the term is $(-1)^\ell$ where ℓ is the number of loops. This establishes that, with our choice of signs for $A_{\alpha\beta}$, the Pfaffian A is precisely the dimer generating function (2) with $n = -1$.

2.3 The free energy

The Pfaffian PfA is the square root of a $2\mathcal{N} \times 2\mathcal{N}$ antisymmetric matrix A. Explicitly, we have

$$Z(-1) = \text{Pf } A = \sqrt{\det A} \tag{3}$$

where

$$\begin{aligned} A &= \begin{pmatrix} 0 & 1 \\ -1 & 0 \end{pmatrix} \otimes I_{N_1} \otimes I_{N_2} \otimes I_{N_3} + \begin{pmatrix} 0 & z \\ -z & 0 \end{pmatrix} \otimes \Big[H_{N_1} \otimes I_{N_2} \otimes I_{N_3} \\ &\qquad + I_{N_1} \otimes H_{N_2} \otimes I_{N_3} + I_{N_1} \otimes I_{N_2} \otimes H_{N_3} \Big]. \end{aligned} \tag{4}$$

Here, I_N is the $N \times N$ identity matrix, H_N is an $N \times N$ matrix given by

$$H_N = \begin{pmatrix} 0 & 1 & 0 & \dots & 0 \\ 0 & 0 & 1 & \dots & 0 \\ \vdots & \vdots & \vdots & \ddots & \vdots \\ 0 & 0 & 0 & \dots & 1 \\ -1 & 0 & 0 & \dots & 0 \end{pmatrix}. \tag{5}$$

Now, H_N can be diagonalized with eigenvalues $e^{i\phi}$, where $\phi = 2\pi n/N$, $n = 1, 2, \cdots, N$. Replacing the H matrices by diagonal ones with its eigenvalues in the diagonal, one obtains

$$Z(-1) = \prod_{n_1=1}^{N_1} \prod_{n_1=1}^{N_2} \prod_{n_3=1}^{N_3} \Big[\det \begin{pmatrix} 0 & 1 + \sum_i z e^{2\pi i n_i/N_i} \\ -1 - \sum_i z e^{-2\pi i n_i/N_i} & 0 \end{pmatrix} \Big]^{1/2}$$

$$= \prod_{n_1=1}^{N_1} \prod_{n_2=1}^{N_2} \prod_{n_3=1}^{N_3} \left| 1 + \sum_{i=1}^{3} z e^{2\pi i n_i / N_i} \right| .$$

This leads to the thermodynamic limit of the free energy

$$f = \frac{1}{(2\pi)^3} \int_0^{2\pi} d\theta_1 \int_0^{2\pi} d\theta_2 \int_0^{2\pi} d\theta_3 \ln \left| 1 + \sum_{i=1}^{3} z e^{i\theta_i} \right| . \tag{6}$$

2.4 The critical behavior

The analysis of the critical behavior of the free energy (6) is facilitated by the use of the integration formula

$$\frac{1}{2\pi} \int_0^{2\pi} d\theta \ln |A + B e^{i\theta}| = \ln \max\{|A|, |B|\} \tag{7}$$

which holds for any complex A and B. We realize bond weights by introducing bond energy ϵ, and write without the loss of generality $z = e^{-\beta\epsilon} < 1$, where $\beta = 1/kT$. Then, multiplying the quantity inside the absolute signs in (6) by $e^{-i\theta_1}$ and carrying out the integration over θ_1, we obtain

$$\begin{aligned} f &= 0, && T < T_c \\ &= \frac{1}{(2\pi)^2} \int d\theta_2 \cdots \int_{\mathcal{R}} d\theta_3 \ln \left| z(1 + \sum_{j=2}^{d} e^{i\theta_j}) \right|, && T > T_c, \end{aligned} \tag{8}$$

where T_c is defined by

$$3z = 1, \tag{9}$$

and the integrations are taken over the regime $\mathcal{R}$ specified by $z|1+e^{i\theta_2}+e^{i\theta_3}| > 1$. Clearly, the free energy is non-analytic in T at T_c with the system frozen below T_c.

To find out the nature of the transition, we evaluate the energy

$$\begin{aligned} U &= -\frac{\partial}{\partial\beta} f(-1) \\ &= \frac{\epsilon}{(2\pi)^2} \left(z \frac{\partial}{\partial z} \right) \int_0^{2\pi} d\theta_1 \int_0^{2\pi} d\theta_2 \ln \max\{z, |x|\} \\ &= \frac{\epsilon}{(2\pi)^2} \int d\theta_1 \int_{\mathcal{R}} d\theta_2 \end{aligned} \tag{10}$$

where

$$x = 1 + z(e^{i\theta_1} + e^{i\theta_2}), \tag{11}$$

and $\mathcal{R}$ is the regime $z > |x|$. In writing out the second line in (10), we have carried out the integration over θ_3. The last line in (10) then follows from the fact that x is independent of z so that the regime $|x| > z$ gives rise to no contribution after taking the derivative.

It is clear that the volume of $\mathcal{R}$ is small near T_c. A detailed analysis[10] shows that

$$U \sim |T - T_c| \tag{12}$$

and hence the critical exponent $\alpha = 0$. Explicitly, one finds

$$\begin{aligned} U &= 0, && T < T_c \\ &= \frac{2\epsilon}{\pi^2} \int_{z-1}^{2z} \frac{du}{\sqrt{4z^2 - u^2}} \cos^{-1}\Big(\frac{1 - u^2 - z^2}{2uz}\Big), && T > T_c \end{aligned} \tag{13}$$

from which one obtains

$$c_v = \frac{dU}{dT} = \frac{3\sqrt{3}}{2\pi} (\ln 3)^2 k, \qquad T \to T_c + . \tag{14}$$

Thus, the specific heat has a cusp singularity at T_c+.

The analysis of this section can be extended to the $O(-1)$ model defined by (1) in d dimensions in which continuous lines run in a preferred direction along all d principal axes of a d-dimensional hypercubic lattice.[9] In this case one again finds the system frozen below T_c, but with T_c defined by $dz = 1$. One also finds the critical exponent $\alpha = (d - 3)/2$.

3 The transfer matrix solution of an interacting layered dimer system

3.1 Definition of the model

Consider a three-dimensional model consisting of K layers of honeycomb dimer lattices. The dimers, which carry weights u, v, w along the three honeycomb0 edge directions, are close-packed within each layer and, in addition, interact between layers. The situation is shown in Fig. 2. For two dimers

Table 1: Dimer interacting energy between two dimers incident at the same site of adjacent layers.

layer $k \to k+1$	w	v	u
w	0	$-2h/3$	$2h/3$
v	$2h/3$	0	$-2h/3$
u	$-2h/3$	$2h/3$	0

incident at the same site in adjacent layers, the interaction energy is given in Table 1.

The two-dimensional honeycomb dimer system can be formulated as a five-vertex model, namely, an ice-rule model with the weights[15]

$$\{\omega_1, \omega_2, \omega_3, \omega_4, \omega_5, \omega_6\} = \{0, w, v, u, \sqrt{uv}, \sqrt{uv}\}. \tag{15}$$

The 5-vertex model is defined on a square lattice of size $M \times N$ mapping to an honeycomb lattice of $2MN$ sites.[15] The mapping is such that the edge state $\alpha = +1$ ($\beta = +1$) corresponds to the presence of a v (u) dimer.

The K layers of $M \times N$ square lattice form a a simple-cubic lattice $\mathcal{L}$ of size $\mathcal{N} = K \times M \times N$ with periodic boundary conditions. Label sites of $\mathcal{L}$ by indices $\{m, j, k\}$, with $1 \le m \le M$, $1 \le j \le N$ and $1 \le k \le K$. Label the state of the horizonal (vertical) edge incident at the site $\{m, j, k\}$ in the direction of, say, decreasing $\{m, j\}$ by α_{mjk} (β_{mjk}). Denote the vertex weight at site $\{m, j, k\}$ by W_{mjk} and the interacting Boltzmann factor between the $\{m, j\}$ sites of two adjacent layers k and $k+1$ by B_{mjk}. It can then be verified that the interaction given in Table 1 can be written in the form of

$$B_{mjk} = \exp\Big(h(\alpha_j \tilde{\beta}_j - \tilde{\alpha}_{j+1}\beta'_j)\Big), \tag{16}$$

where for convenience we have suppressed the subscripts m and k and introduced the notation

$$\beta_{m+1,j,k} \to \beta'_j, \qquad \beta_{m,j,k+1} \to \tilde{\beta}_j, \tag{17}$$

and similarly for the α's. Note that as a consequence of the ice rule the

quantity

$$y_k = \frac{1}{N}\sum_{j=1}^{N}\beta_j = \frac{1}{N}\sum_{j=1}^{N}\beta'_j \tag{18}$$

is conserved within each layer and is independent of m.

The problem at hand now is the evaluation of the partition function

$$Z_{MNK} = \sum_{\alpha_{mjk}}\sum_{\beta_{mjk}}\prod_{k=1}^{K}\prod_{m=1}^{M}\prod_{j=1}^{N}\Big(B_{mjk}W_{mjk}\Big) \tag{19}$$

where the summations are taken over all edge states α_{mjk} and β_{mjk}, and the per-site "free energy"

$$f = \lim_{M,N,K\to\infty}(MNK)^{-1}\ln Z_{MNK}. \tag{20}$$

3.2 The transfer matrix

The partition function (19) can be evaluated by applying a transfer matrix in the vertical direction. In a horizontal cross section of $\mathcal{L}$ there are NK vertical edges. Let $\{\beta_m\} = \{\beta_{mjk}|1 \le j \le N, 1 \le k \le K\}$, $1 \le m \le M$ denote the states of these NK vertical edges, and define a $2^{NK}\times 2^{NK}$ matrix $\mathbf{T}$ with elements

$$T(\{\beta_m\},\{\beta_{m+1}\}) = \sum_{\alpha_{mjk}}\prod_{k=1}^{K}\prod_{j=1}^{N}(B_{mjk}W_{mjk}). \tag{21}$$

Then one has

$$Z_{MNK} = \sum_{\beta_{mjk}}\prod_{m=1}^{M}T(\{\beta_m\},\{\beta_{m+1}\}) \sim \Lambda_{\max}^{M}, \tag{22}$$

where $\Lambda_{\max}$ is the largest eigenvalue of $\mathbf{T}$. The validity of the ice rule within each layer now permits one to use a global Bethe ansatz in the analysis.

The interlayer interaction (16) leads to a considerable simplification of the transfer matrix. It can be shown[11] that we have

$$\prod_{m=1}^{M}\prod_{j=1}^{N}B_{mjk} = \prod_{m=1}^{M}\exp\Big[Nh(\alpha_{m,1,k}y_{k+1} - \alpha_{m,1,k+1}y_k)\Big]. \tag{23}$$

As a result, only the conserved quantities y_k and the state $\alpha_{m,1,k}$ appear in the final product. This leads us to recast the partition function (19) in the form of

$$\begin{aligned} Z_{MNK} &= \sum_{\beta_{mjk}} \prod_{m=1}^{M} T^{\rm eff}(\{\beta_m\},\{\beta_{m+1}\}) \\ &= {\rm Tr}(\mathbf{T}^{\rm eff})^M \end{aligned} \tag{24}$$

with

$$T^{\rm eff}(\{\beta_m\},\{\beta_{m+1}\}) = \sum_{\alpha_{mjk}} \prod_{k=1}^{K} \Big(e^{Nh\alpha_{m,1,k}(y_{k+1}-y_{k-1})} \prod_{j=1}^{N} W_{mjk} \Big). \tag{25}$$

The problem is now reduced to one of finding the largest eigenvalue of the matrix $\mathbf{T}^{\rm eff}$ with matrix elements as shown. The task is now considerably simpler since one needs only to keep track of two-dimensional systems.

3.3 The free energy

The eigenvalues of the effective matrix are obtained by applying a global Bethe ansatz consisting of the usual Bethe ansatz for each layer. The algebra is straightforward and the result is

$$Z_{MNK} \sim \max_{\{n_k\}} \prod_{k=1}^{K} [\Lambda_L(n_k)]^M, \tag{26}$$

with

$$\Lambda_L(n_k) = e^{2h(n_{k+1}-n_{k-1})} \omega_4^{N-n_k} \prod_{j=1}^{n_k} \Big[\frac{\omega_2\omega_4 + \omega_5\omega_6 z_j^{(k)}}{\omega_4} \Big] \tag{27}$$

being the eigenvalue for $\alpha_{m,1,k} = -1$ and, for each $1 \le k \le K$, the n_k complex numbers $z_j^{(k)}$ are

$$z_j^{(k)} = e^{i\theta_j} e^{2h(y_{k+1}-y_{k-1})}, \quad j = 1, 2, \cdots, n_k \tag{28}$$

where $e^{i\theta_j}$ are n_k distinct Nth roots of $(-1)^{n_k+1}$. Using (15) and (20), this leads to the per-site free energy

$$\begin{aligned} f &= \ln u + \lim_{K\to\infty} \max_{-1\le y_k\le 1} \frac{1}{K} \sum_{k=1}^{K} \frac{1}{2\pi} \int_{-\pi(1-y_k)/2}^{\pi(1-y_k)/2} \\ &\quad \times \ln\Big(\frac{w}{u} + \frac{v}{u} e^{2h(y_{k+1}-y_{k-1})} e^{i\theta} \Big) d\theta. \end{aligned} \tag{29}$$

3.4 The phase diagram

Analyses of the free energy (29) lead to the following:[11] For large u, v or w, the system is frozen with complete ordering of u, v, or w dimers in all layers, and hence the free energies

$$\begin{aligned} f_U &= \ln u, && U \text{ phase} \\ f_V &= \ln v, && V \text{ phase} \\ f_W &= \ln w, && W \text{ phase.} \end{aligned} \tag{30}$$

These are referred to as the U, V, and W phases, respectively. For large h, it is seen from Table 1 that the energetically preferred state is the one in which each layer is occupied by one kind of dimers, u, v, or w, and that the layers are ordered in the sequence of $\{u, w, v, u, w, v \cdots\}$. This ordered phase is referred to as the H phase with the free energy

$$f_H = \frac{1}{3}\ln(uvwe^{4h}), \qquad H \text{ phase.} \tag{31}$$

More generally one finds that the extremum value in (29) always repeats in multiples of 3, namely, with

$$y_{k+3} = y_k.$$

The following extremum sets of $\{y_k\}$ are found:

1. $\{y_1, y_2, y_3\} = \{1, 1, 1\}$: In this case we have all $y_k = 1$, and hence from (29)

$$f = f_U, \qquad U \text{ phase.} \tag{32}$$

2. $\{y_1, y_2, y_3\} = \{-1, -1, -1\}$: In this case we have all $y_k = -1$, and hence from (29)

$$\begin{aligned} f &= \ln u + \frac{1}{\pi}\int_0^\pi \ln\left|\frac{w}{u} + \frac{v}{u}e^{i\theta}\right| d\theta \\ &= f_W, \qquad w > v \qquad W \text{ phase} \\ &= f_V, \qquad v > w. \qquad V \text{ phase} \end{aligned} \tag{33}$$

3. $\{y_1, y_2, y_3\} = \{1, -1, -1\}$: Substituting this sequence of y_k values into (29) and making use of the integration formula (7) in the resulting expression, one

obtains

$$\begin{aligned} f &= \ln u + \frac{1}{6\pi}\int_{-\pi}^{\pi} \ln\left|\frac{w}{u} + \frac{v}{u}e^{2h}e^{i\theta}\right| d\theta + \frac{1}{6\pi}\int_{-\pi}^{\pi} \ln\left|\frac{w}{u} + \frac{v}{u}e^{-2h}e^{i\theta}\right| d\theta \\ &= \frac{1}{3}f_U + \frac{2}{3}f_W, \qquad ve^{-4h} < ve^{4h} < w \\ &= \frac{1}{3}f_U + \frac{2}{3}f_V, \qquad w < ve^{-4h} < ve^{4h} \\ &= f_H. \qquad ve^{-4h} < w < ve^{4h}. \end{aligned} \tag{34}$$

Now the free energies in the second and third lines can be discarded since they are always smaller than the largest of $\{f_U, f_V, f_W\}$. Thus, this set of $\{y_k\}$ leads to a frozen ordering for sufficiently large h as indicated in the last line.

4. $\{y_1, y_2, y_3\} = \{y, y, y\}$: In this case all $y_k = y$, y maximizes the free energy (29). Then, substituting $y_k = y$ into (29) and carrying out a straightforward differentiation with respect to y, one obtains

$$f = f_Y(y_0), \qquad Y \text{ phase} \tag{35}$$

where the extremum y_0 is given by

$$\frac{\pi}{2}(1 - y_0) = \cos^{-1}\left[\frac{u^2 - w^2 - v^2}{2wv}\right]. \tag{36}$$

This is a disorder phase which we refer to as the Y phase.

5. $\{y_1, y_2, y_3\} = \{y_1, -1, -1\}$: This is the H phase with the u layers replaced by layers with $y_k = y_1$, so that the layer ordering is $\{y_1, w, v, y_1, w, v \cdots\}$. This is a partially ordered phase which we refer to as the I_u phase.

6. $\{y_1, y_2, y_3\} = \{1, y_2, -1\}$: This is the H phase with the w layers replaced by layers with $y_{k+1} = y_2$, so that the layer ordering is $\{u, y_2, v, u, y_2, v \cdots\}$. We refer to this as the I_w phase.

7. $\{y_1, y_2, y_3\} = \{1, -1, y_3\}$: This is the H phase with the v layers replaced by layers with $y_{k+2} = y_3$, so that the layer ordering is $\{u, w, y_3, u, w, y_3 \cdots\}$. We refer to this as the I_v phase.

Since the phase diagram must reflect the $\{u, v, w\}$ symmetry of the interlayer interaction given in Table 1, it is convenient to introduce coordinates

$$X = \ln(v/w) \qquad Y = (\sqrt{3})^{-1}\ln(vw/u^2) \tag{37}$$

such that any interchange of the three variables u, v, and w corresponds to a 120° rotation in the $\{X, Y\}$ plane. The phase boundaries are then determined by equating the free energies of adjacent phases. The results are collected in Fig. 3. One finds the following:

• $h < h_0$: For small h the phase diagram is the same as that of the $h = 0$, the diagram shown in Fig. 3(a). The phase boundaries between the $\{U, V, W\}$ phases and the Y phase are

$$u = |v \pm w|. \tag{38}$$

• $h_0 < h < h_1$: As h increases from zero, our numerical analyses indicate that the H phase appears when h reaches the value

$$h_0 = \frac{3}{8\pi} \int_0^{2\pi/3} \ln(2 + 2\cos\theta) d\theta = 0.2422995.... \tag{39}$$

The resulting phase diagram is shown in Fig. 3(b). The phase boundary between the H and Y phases is

$$\frac{1}{3} \ln(uvwe^{4h}) = f_Y(y_0). \tag{40}$$

• $h_1 < h < h_2$: As h increases from h_0, the I_u, I_v, I_w phases appears when h reaches a certain value h_1. The resulting phase diagram is shown in Fig. 3(c). The numerical value of h_1 is given by

$$h_1 = \frac{1}{4} \ln\Big(\frac{2v}{u}\Big) = 0.2552479\cdots,$$

where v/u is the solution of the two equations

$$(1 + y_0) \ln \frac{v}{u} + \frac{1}{6}(1 + 3y_0) \ln 2 = \frac{1}{\pi} \int_0^{\pi(1-y_0)/2} \ln(1 + \cos\theta) d\theta \tag{41}$$

$$\frac{\pi}{2}(1 - y_0) = \cos^{-1}\Big(\frac{u^2}{2v^2} - 1\Big). \tag{42}$$

• $h_2 < h < h_3$: As h increases from h_1, it was found that the regimes I_u, I_v, and I_w extends to infinite when h exceeds the value

$$h_2 = (\ln 3)/4 = 0.2746530\cdots.$$

The phase diagram is shown in Fig. 3(d).

• $h_3 < h < h_4$: As h increases from h_2, it was found that the boundary of the H phase bulges toward the U, V, W phases along the $30°, 150°, 270°$ lines, touching the U, V, W boundaries in these directions when h equals to

$$h_3 = (\ln 2)/2 = 0.3465735\cdots.$$

For $h > h_3$, the H phase borders directly with the U, V, W phases with respective boundaries

$$u^2 = vwe^{4h}, v^2 = wue^{4h}, w^2 = uve^{4h}. \tag{43}$$

The size of these borders grows while the Y phase shrinks as h increases. The phase diagram in this regime is shown in Fig. 3(e).

• $h > h_4$: As h increases further from h_3, it was found that the Y phase disappears completely when h exceeds the value

$$h_4 = \frac{1}{8}\ln(1+\gamma^2) = 0.3816955\cdots,$$

where γ is the solution of the equation

$$\gamma - \tan^{-1}\gamma = \pi. \tag{44}$$

3.5 The critical behavior

The critical behavior near all phase boundaries can be analyzed by expanding the free energy. We find all transitions to be of first order, except those between the $\{U, V, W\}$ and Y phases, and between the $\{I_u, I_v, I_w\}$ and H phases, which are shown below to be the same as that in the 5-vertex model,[15, 16] namely, a continuous transition with a square-root singularity in the specific heat. This transition, first reported by this author[16] in 1967, is now more widely known as the Pokrovsky-Talapov type phase transition.[17]

To see the occurrence of the Pokrovsky-Talapov type transitions, we note that the ordered U, V, W and H phases (with $y_k = \pm 1$) have constant free energies and hence zero first derivatives. The transition between the U, V, W phases and the Y phase is the same as in two dimensions, and is

continuous.[15] This fact can be seen by expanding the free energy near y_0 as

$$\begin{aligned} f_Y(y) &= f_Y(y_0) + (y-y_0)f'_Y(y_0) + \frac{1}{2!}(y-y_0)^2 f''_Y(y_0) \\ &\quad + \frac{1}{3!}(y-y_0)^3 f'''_Y(y_0) + \cdots . \end{aligned} \tag{45}$$

Using the expression of $f_Y(y)$ given by (35), one sees that, indeed, the first derivative $f_Y(y_0)$, $y_0 = \pm 1$, vanishes identically on the boundary (38) which is precisely $f'_Y(y_0) = 0$. Furthermore, it is also seen that $f''_Y(y_0) \sim \sin[\pi(1 - y_0)/2] = 0$. Therefore, the extremum of $f_Y(y)$ given by (45) occurs at $y = y_{\rm extrm}$ determined from

$$y_{\rm extrm} - y_0 = \pm \sqrt{\frac{2f'_Y(y_0)}{-f'''_Y(y_0)}} \sim t^{1/2}, \tag{46}$$

where $t = |T - T_c|$, T_c being the critical temperature. Substituting this $y_{\rm extrm}$ into (45), one obtains

$$\begin{aligned} f_Y(y_{\rm extrm}) &= f_Y(y_0) \pm \frac{2}{3} f'_Y(y_0) \sqrt{\frac{2f'_Y(y_0)}{-f'''_Y(y_0)}} \\ &= f_Y(y_0) + c(u,v,w,h)t^{3/2}. \end{aligned} \tag{47}$$

This leads to a square-root singularity in the specific heat.

Applying the same analysis to the H and I_u phases, one concludes

$$f_{I_u}(y_{\rm extrm}) = f(y_{10}) + c_1(u,v,w,h)t^{3/2}. \tag{48}$$

This gives rise again to a square-root singularity in the specific heat.

4 Summary

We have described the exact solutions of two lattice models in three dimensions, an $O(-1)$ model solved using the combinatorial method of Pfaffians, and a layered dimer model solved using an algebraic transfer matrix. However, both models stop short of being genuinely three-dimensional. The

$O(-1)$ model suffers two defects. First, it describes line configurations running only in preferred directions. Secondly, the Boltzmann weights can be negative. The solution of a model without these restrictions would help us to solve the Ising model in three dimensions. The layered dimer model, while having strictly positive weights, describes dimer configurations in which dimers are confined in planes. As a consequence, the critical behavior is essentially two-dimensional.

Acknowledgments

This work is supported in part by NSF grant DMR-9614170.

References

[1] E. Ising, *Z. Physik* **31**, 253 (1925).

[2] L. Onsager, *Phys. Rev.* **65**, 117 (1944).

[3] E.H. Lieb, *Phys. Rev. Lett.* **18**, 692, 1046 (1967); **19**, 108, (1967).

[4] See, for example, E.H. Lieb and F.Y. Wu, in *Phase Transitions and Critical phenomena* Vol. I, Eds. C. Domb and M.S. Green (Academic Press, New York 1972).

[5] See, for example, R.J. Baxter, Exactly Solved Models in Statistical Mechanics (Academic Press, London, 1982).

[6] A.B. Zamolodchikov, *JETP* **52**, 325 (1980).

[7] R.J. Baxter, *Commun. Math. Phys.* **88**, 185 (1983).

[8] V.V. Bazhanov and R.J. Baxter, *J. Stat. Phys.*, **69**, 453 (1992).

[9] F.Y. Wu and H.Y. Huang, *Lett. Math. Phys.*, **29**, 205 (1993).

[10] H.Y. Huang, V. Popkov, and F.Y. Wu, *Phys. Rev. Lett.* **78**, 409 (1997).

[11] V. Popkov, D. Kim, H.Y. Huang, and F.Y. Wu, *Phys. Rev.* E **56**, 3999 (1997).

[12] B. Nienhuis, *Phys. Rev. Lett.* **49**, 1062 (1982).

[13] B. Nienhuis, *J. Stat. Phys.* **34**, 731 (1984).

[14] P.W. Kasteleyn, *Physica* **27**, 1207 (1961).

[15] F.Y. Wu, *Phys. Rev.* **168** 539 (1968).

[16] F.Y. Wu, *Phys. Rev. Lett.* **19**, 103 (1967).

[17] V.L. Pokrovsky and A.L. Talapov, *Phys. Rev. Lett.* **42**, 65 (1979).

Figure captions

Fig. 1. (a) A lattice point of the simple cubic lattice $\mathcal{L}$. (b) The split of the lattice point in (a) into two points.

Fig. 2. A stack of K layers of honeycomb dimmer lattices.

Fig. 3. The phase diagram.

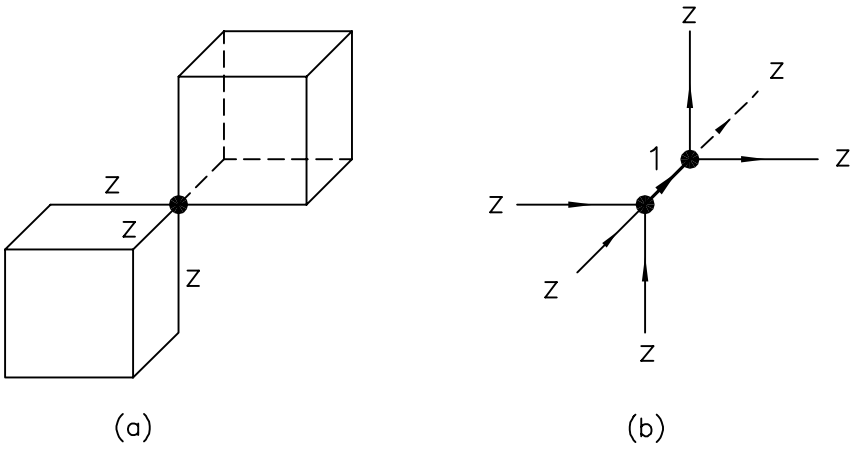

(a) (b)

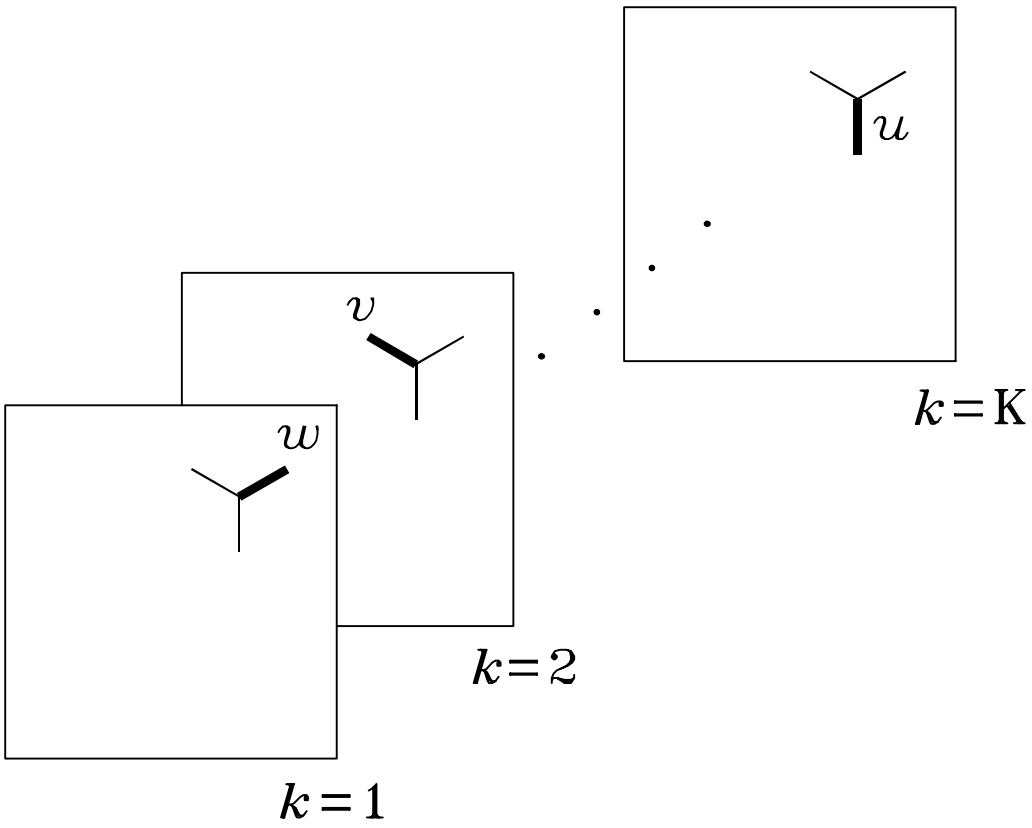

Fig. 2

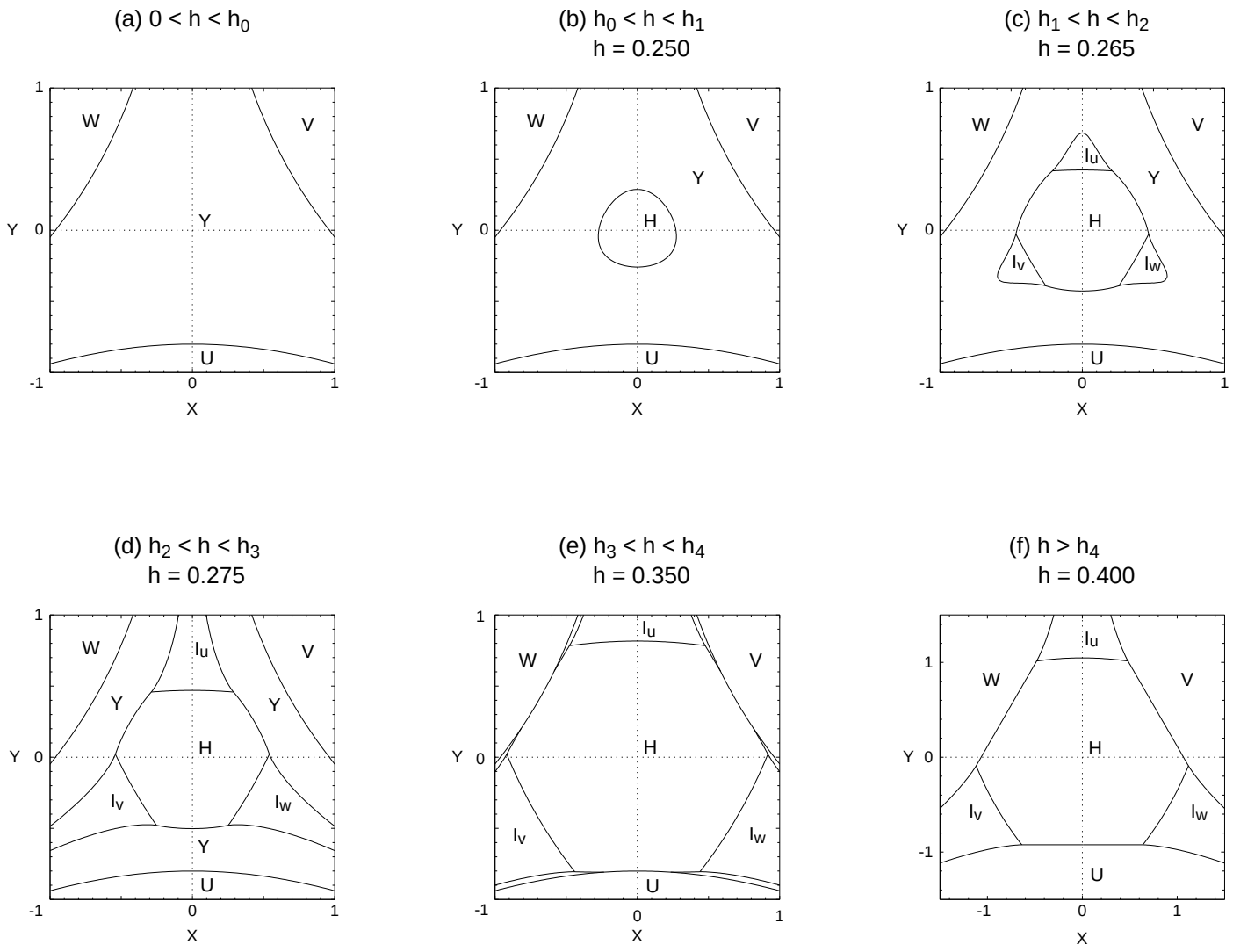
(a) 0 < h < h0
(b) h0 < h < h1
h = 0.250
(c) h1 < h < h2
h = 0.265
(d) h2 < h < h3
h = 0.275
(e) h3 < h < h4
h = 0.350
(f) h > h4
h = 0.400
W
V
Y
H
U
Iu
Iv
Iw
X
Y
1
0
-1

Fig. 3